Mechanism for linear and nonlinear optical effects in crystals of the $Sr_2Be_2B_2O_7$ family

Zheshuai Lin, Zhizhong Wang, and Chuangtian Chen[a)]
Beijing Center of Crystal R&D, Technical Institute of Physics and Chemistry, Chinese Academy of Sciences, P.O. Box 2711, Beijing 100080, China

Shyong K. Chen and Ming-Hsien Lee
Department of Physics, Tamkang University, Tamsui, Taipei 251, Taiwan

(Received 3 December 2002; accepted 3 April 2003)

Electronic structure calculations of $Sr_2Be_2B_2O_7$ (SBBO) family crystals including $Sr_2Be_2B_2O_7$, $BaAl_2B_2O_7$, and $K_2Al_2B_2O_7$ have been performed based on a plane-wave pseudopotential method. Moreover, the linear optical coefficients and the static second-harmonic generation (SHG) coefficients of $BaAl_2B_2O_7$ and $K_2Al_2B_2O_7$ are calculated at the independent-particle level. The calculated refractive indices and SHG coefficients are in good agreement with experimental values. In addition, a real-space atom-cutting method is adopted to analyze the respective contributions of the cations and anionic group to optical response. The results show that in these crystals, when the radii of the cations increase, their contributions to the SHG effect become slightly more pronounced, however, the contributions to the SHG coefficients from the $(BO_3)^{3-}$ and $(AlO_4)^{5-}$ anionic groups are dominant and comparable. © *2003 American Institute of Physics.* [DOI: 10.1063/1.1577816]

I. INTRODUCTION

It is well known that a laser in the ultraviolet (UV) region would be very useful for a wide range of applications, such as photolithography, micromachining, and data storage. The search for potential UV nonlinear optical (NLO) crystals has been in progress for more than 30 years. Our group has used a molecular engineering approach[1] to search for new NLO crystals in borate-based compounds. As a result, a series of crystals such as $Sr_2Be_2B_2O_7$ (SBBO) (Ref. 2) and $BaAl_2B_2O_7$ (BABO),[3,4] which were reported by Yamada,[3] and $K_2Al_2B_2O_7$ (KABO) (Refs. 5–7) were discovered during the 1990s. Recently, a beam at 266 nm has been obtained by fourth-harmonic generation of 1064 nm Nd:YAG laser radiation through a KABO crystal[8] with optical conversion efficiency from 532 to 266 nm of 13%, which promises to be an excellent prospect for applications in the UV region.

The space structures of BABO and KABO are very similar to that of SBBO, thus they all belong to the SBBO family. The experimental linear and nonlinear optical parameters of the latter are given in Table I. To understand the mechanism for producing second-harmonic generation (SHG) in the SBBO family, anionic group theory,[1] a localized quantum-chemistry model, was used. However, a more comprehensive understanding can only be achieved by performing an *ab initio* energy band structure calculation, in which the influence of cations on the band structure and optical response can be directly evaluated.

Recently, we employed CASTEP,[9] a plane-wave pseudopotential total energy package, to calculate the electronic band structures and linear and nonlinear optical properties of the BBO and LBO family.[10,11] In addition, a real-space atom-cutting method has been suggested to analyze the respective contributions of various transitions among cations and anionic groups to the optical responses of BBO and LBO family crystals. The results indicate that the contributions of cations to SHG become slightly more pronounced with an increase of their radii in the same family of crystals. In other words, the major contributions to the SHG coefficients and birefringence still come from the $(B_3O_6)^{3-}$ and $(B_3O_7)^{5-}$ anionic groups in the BBO and LBO family. In this article we use the same calculation method to analyze the electronic band structures and the mechanism for the linear and nonlinear optical properties of the SBBO family and obtain some useful results which are essential to the design and search for new NLO crystals.

II. METHODS AND COMPUTATIONAL DETAILS

The theoretical basis of CASTEP is the local-density approximation (LDA)[12] or gradient-corrected LDA[13] based on density functional theory (DFT).[14] Within such a framework, the preconditioned conjugated gradient (CG) band-by-band method[15] used in CASTEP ensures a robust efficient search of the energy minimum of the electronic structure ground state. The optimized pseudopotentials[16–18] in Kleinman–Bylander form[19] for K, Ba, Sr, Al, Be, B, and O allow us to use a small plane-wave basis set without compromising the accuracy required by our study. For example, $5s$ and $5p$ together with $6s$ electrons of Ba are treated as valence electrons in the pseudopotential to ensure that Ba is described accurately enough without applying nonlinear core correction.

It is well known that the band gap calculated by the LDA is usually smaller than the experimental data due to the discontinuity of exchange-correlation energy. A scissors operator[20,21] is also used to shift upward all the conduction bands in order to agree with measured values of the band gap.

[a)]Electronic mail: cct@cl.cryo.ac.cn

TABLE I. Transport range and nonlinear optical parameters of SBBO, BABO, and KABO crystals.

Crystal	Point group	Transparent range (nm)	d_{ij} (pm/V)
SBBO[a]	D_{3h}	165–3780	$d_{22}=1.62$
BABO[b]	D_3	≈200–3780	$d_{11}=0.75$
KABO[c]	D_3	≈180–3780	$d_{11}=0.48$

[a]Reference 2.
[b]Reference 3.
[c]Reference 4.

The static limit of the SHG coefficients plays the most important role in the application of SHG crystals. Our group and collaborators have reviewed various calculation methods for SHG coefficients,[10] and improved the formula presented by Rashkeev *et al.*[22] to calculate them,

$$\chi^{\alpha\beta\gamma}=\chi^{\alpha\beta\gamma}(VE)+\chi^{\alpha\beta\gamma}(VH)+\chi^{\alpha\beta\gamma}\ \text{(two bands)},$$

where $\chi^{\alpha\beta\gamma}(VE)$ and $\chi^{\alpha\beta\gamma}(VH)$ contribute to $\chi_i^{(2)}$ through virtual-electron processes and virtual-hole processes, respectively; $\chi^{\alpha\beta\gamma}$ (two bands) is the contribution to $\chi_i^{(2)}$ from the two-band processes. The formulas for calculating $\chi^{\alpha\beta\gamma}(VE)$, $\chi^{\alpha\beta\gamma}(VH)$, and $\chi^{\alpha\beta\gamma}$ (two bands) are given in Ref. 10.

To investigate the influence of the ions on the crystal's optical response, a real-space atom-cutting method has been used. With this method the contribution of ion A to the nth-order susceptibility denoted as $\chi^{(n)}(A)$ is obtained by cutting all ions except A from the original wave functions $\chi^{(n)}(A)=\chi^{(n)}$ (all ions except A are cut).

The geometric parameters of SBBO, BABO, and KABO are as follows: SBBO ($6m2$, $a=b=4.683$ Å, $c=15.311$ Å, $\alpha=\beta=90°$, $\gamma=120°$),[2] BABO ($R32$, $a=b=5.001$ Å, $c=24.378$ Å, $\alpha=\beta=90°$, $\gamma=120°$),[4] and KABO ($P321$, $a=b=8.530$ Å, $c=8.409$ Å, $\alpha=\beta=90°$, $\gamma=120°$).[5]

The basic structural features of the SBBO, BABO, and KABO crystals are shown in Fig. 1. Their unit cells contain 2, 3 and 3 formula units, and 26, 36 and 39 atoms, respectively. Figure 1 clearly shows that the nearly planar $(Be_3B_3O_6)$ or $(Al_3B_3O_6)$ network perpendicular to the c axis with three terminal O atoms all of $(BO_3)^{3-}$ groups linked with the nearest neighbors and the $(BO_3)^{3-}$ group maintains a coplanar configuration. Binding between the $(Be_3B_3O_6)$ or $(Al_3B_3O_6)$ layers is strong, since they are bridged by oxygen atoms bound to Be or Al atoms. The crystals of the SBBO family are easier to grow and have better mechanical properties than those of the $KBe_2BO_3F_2$ (KBBF) crystal which has a strong layering tendency within its structure.[1] On the other hand, these structural arrangements are different from the space structures of BBO, in which the $(B_3O_6)^{3-}$ group is a basic structural unit, and the LBO family, in which an additional tetrahedral coordinated B appears. In addition to the $(BO_3)^{3-}$ group, the SBBO family has the other anionic group $(BeO_4)^{6-}$ or $(AlO_4)^{5-}$.

All these structural factors should have a specific influence on the electronic and band structures of SBBO, BABO, and KABO crystals, and consequently on their optical properties. An *ab initio* pseudopotential calculation can reveal the effects in a straightforward manner. With the real-space atom-cutting method, the respective actions of the anionic groups and cations (K^+,Sr^{2+},Ba^{2+}) on the optical properties may be recognized and understood. This is the goal of this article.

III. RESULTS AND DISCUSSION

A. Band structure

The energy bands of SBBO, BABO, and KABO crystals were calculated. It is worth noting that the calculated band gap of SBBO is much smaller than that of BABO or KABO, whereas its experimental cutoff frequency is higher. We believe that this is because the structure of the SBBO crystal is in an unstable phase in which the positions of the oxygen atoms are statistically distributed and difficult to determine

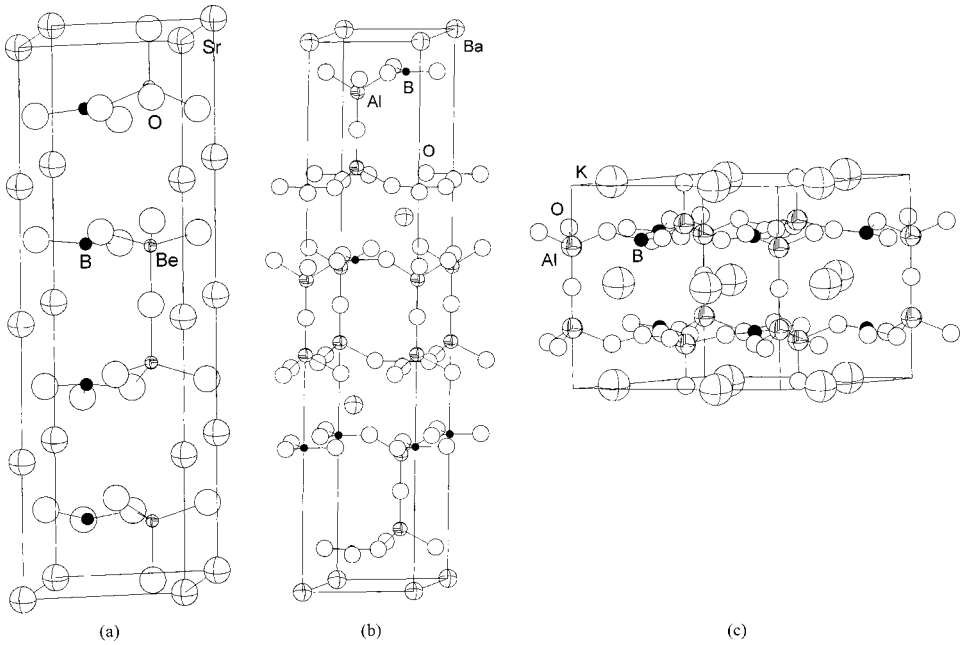

FIG. 1. Unit cell of the SBBO family: (a) SBBO, (b) BABO, and (c) KABO.

properly by experiment, since its structural convergence factor is larger than 0.065.[2] This unstable structure of SBBO leads to an abnormally small calculated energy gap, and eventually results in a large difference in calculated optical properties and experimental values. Hence we will not further analyze or discuss the energy bands and related calculations of the optical properties of SBBO.

The calculated band structures of BABO and KABO in the unit cell plotted along the lines of symmetry are shown in Figs. 2(a) and 2(b), respectively. It can be seen that each band structure is divided into three regions. The lower region is located below -15 eV, and mainly consists of $2s$ orbitals of oxygen atoms. The middle region is the valence band (VB) from about -10 to 0 eV and may be separated into two pieces, the lower one of which is very flat. The upper one is the conduction band (CB) with a total width of about 5 eV. The calculated band gaps of BABO and KABO are 3.755 and 3.240 eV, respectively, and are smaller than in the corresponding experimental data (6.186 and 6.870 eV, respectively). In DFT, although the calculated band gap does not correspond to the experimental energy band gap in the quasiparticle picture, the energy band profiles are correct, especially those for the valence bands. We have also used other kinds of pseudopotentials to calculate the bands and found no obvious changes in the results.

Figures 3(a) and 3(b) give the total density of states (DOS) and partial DOS (PDOS) projected onto the constitutional atoms of BABO and KABO crystals, respectively. In addition, as an example, Fig. 4 shows the orbital-resolved PDOS in BABO crystal (aluminum and boron are not shown because the contributions of their orbital components are all less than 0.5 or almost zero). Several characteristics can be seen from the DOS and PDOS in Fig. 3. (1) The orbitals of the aluminum atom have almost no contribution to the bands of BABO and KABO. (2) The bands lower than -15 eV mostly consist of $2s$ orbitals of oxygen atoms of both $(BO_3)^{3-}$ and $(AlO_4)^{5-}$. In fact, the $2s$ orbitals of the oxygen atoms are strongly localized at -17 eV. (3) The valence bands are mainly composed of $2p$ orbitals of oxygen atoms in both $(BO_3)^{3-}$ and $(AlO_4)^{5-}$, but for BABO the $5p$ semicore states of the Ba^{2+} cation are located in a band centered at -10 eV. In addition, a peak of the p orbitals of the K^+ cation occurs at about -10 eV in KABO. At the very top of the VB (from 0 to -3 eV), there is no obvious hybridization between the orbitals of B and O atoms. (4) The conduction bands of the two crystals are mainly composed of valence orbitals of O and B atoms.

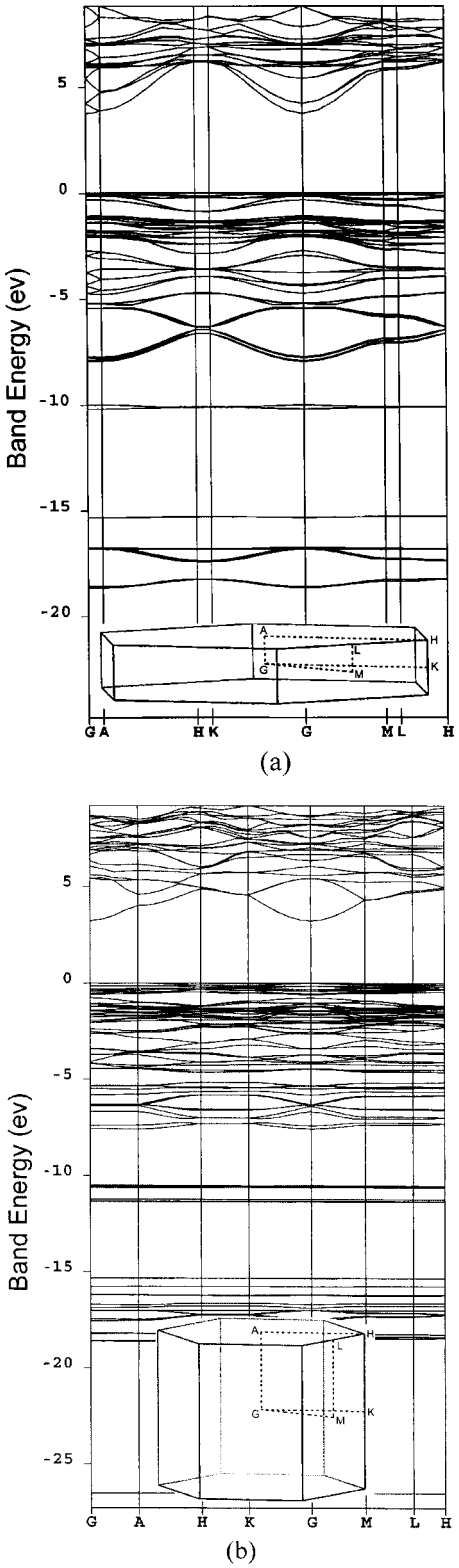

FIG. 2. Band structure of BABO and KABO: (a) BABO and (b) KABO.

B. Linear optical susceptibility

It is well known that the refractive indices are obtained theoretically from the dielectric constants. The real part of the dielectric function can be obtained from its imaginary part using the Kramers–Kronig transformation. The imaginary part can be calculated with the matrix elements that describe the electronic transitions between the ground and excited states in the crystals considered. The calculation formulas are given in Ref. 10. The calculated and experimental values of refractive indices at 1064 nm wavelengths are listed in Table II. To investigate the frequency dependence of the dielectric function, as an example the calculated and experimental refractive indices as a function of different frequencies are shown in Fig. 5 for the KABO crystal.

To investigate the influence of the ions on the optical response of BABO and KABO, the atom-cutting method is used. Figure 6 presents the charge-density distribution in the

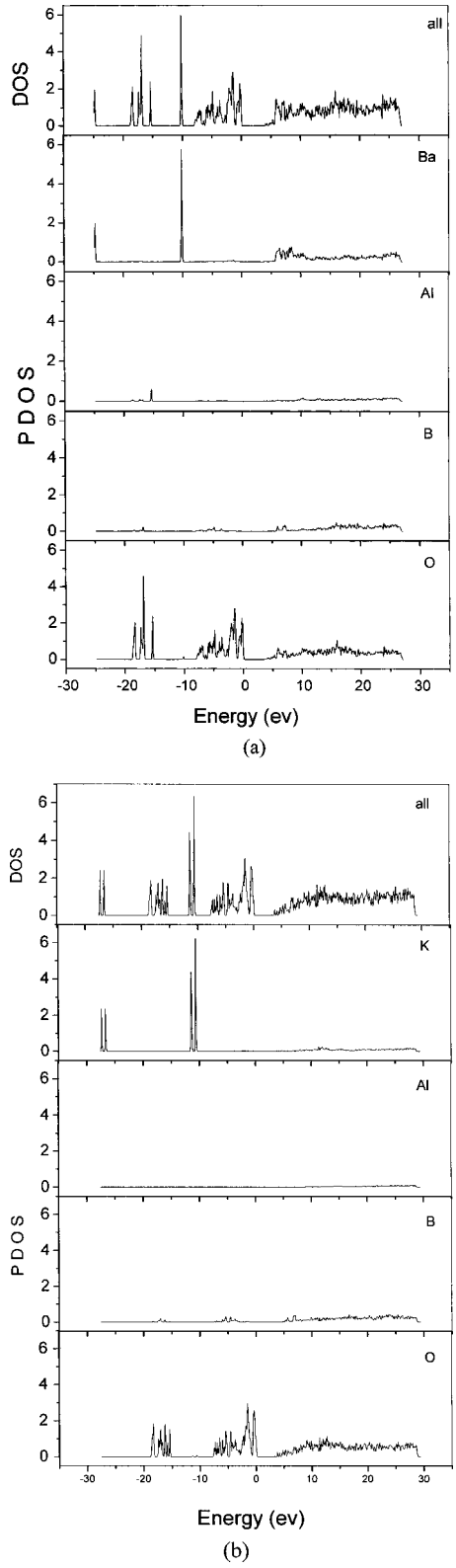

FIG. 3. DOS and PDOS plots of BABO and KABO: (a) BABO and (b) KABO.

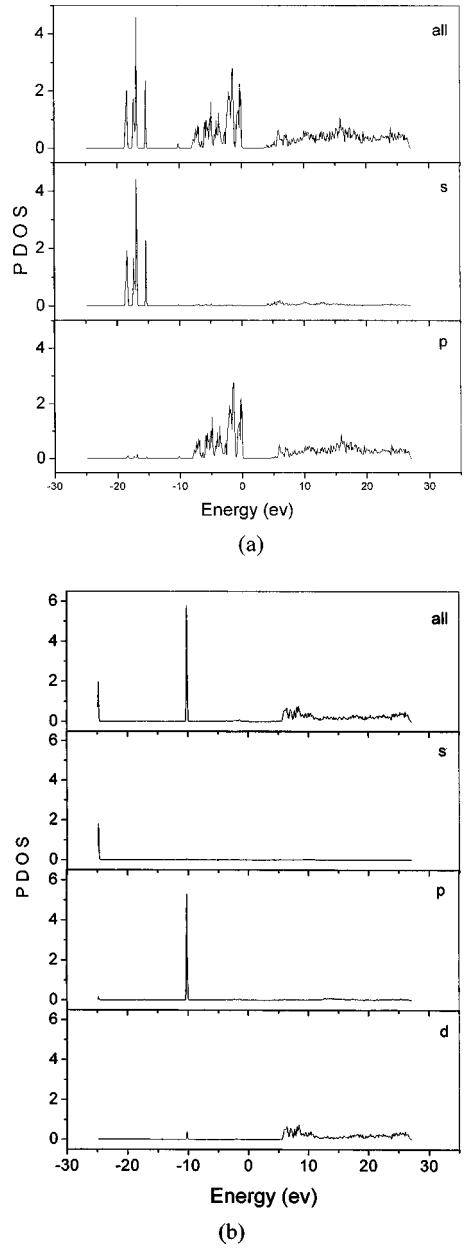

FIG. 4. Orbitally resolved PDOS plot for BABO: (a) O and (b) Ba.

plane of the $(BO_3)^{3-}$ group of BABO as an example. We find that the distance between B and O in the $(BO_3)^{3-}$ group is much smaller than that between Ba^{2+} (or K^+ for KABO) and the $(BO_3)^{3-}$ group. In addition, the charge density in the $(BO_3)^{3-}$ group is relatively delocalized compared to that of the Ba^{2+} (or K^+) cation. This indicates that the bonding between B and O is more covalent. It is therefore difficult to separate the B and O ions, and the $(BO_3)^{3-}$ group should be treated as a whole. The situation for $(AlO_4)^{5-}$ is similar to that of $(BO_3)^{3-}$ group, so we should account for the respective contributions of Ba^{2+} (K^+), $(BO_3)^{3-}$, and $(AlO_4)^{5-}$ to the optical properties.

In a previous paper[10] it was found that the charge density around cation (M) is spherical. Thus we first choose the cutting radii of K and Ba as 1.40 and 1.50 Å, respectively. Following the rule of keeping the cutting spheres of M and O in contact and not overlapped, the cutting radius of O is set at 1.10 Å. For the aluminum atom the cutting radius is chosen as 0.90 Å. Finally, a covalent radius of 0.88 Å of B is chosen as its cutting radius.

The atom-cutting analysis results are given in Table III. The conclusions from the above calculations are as follows:

TABLE II. Calculated and experimental values of refractive indices of SBBO, BABO, and KABO crystals at 1.064 μm.

	Calculated			Experiment		
Crystal	n_0	n_e	Δn	n_0	n_e	Δn
SBBO[a]	1.6920	1.6401	0.052	1.698	1.636	0.062
BABO[b]	1.5757	1.5257	0.050	1.570	1.517	0.053
KABO[c]	1.5590	1.5071	0.052	1.560	1.492	0.068

[a]Experimental values reported in Ref. 2.
[b]Experimental values reported in Ref. 3.
[c]Experimental values reported in Ref. 4.

(i) The calculated refractive indices are in good agreement with the experimental values (the relative error is less than 3%–5%). For the two crystals considered, the theoretical birefringence Δn is also in excellent agreement with the experimental values. The agreement proves the validity of our investigations of BABO and KABO with the pseudopotential method. The results should be very helpful for designing NLO crystals. (ii) Table III shows that for BABO and KABO the contributions of K^+ and Ba^{2+} to the refractive indices are comparable to those of $(BO_3)^{3-}$ and $(AlO_4)^{5-}$ groups, but their contributions to the anisotropy of refractive indices can be neglected. Moreover, we can easily find that although the contribution of the $(AlO_4)^{5-}$ group to refractive indices is comparable to that of the $(BO_3)^{3-}$ group, its contribution to birefringence is much smaller than that of $(BO_3)^{3-}$. The results are consistent with those obtained by anionic theory.[1]

C. SHG coefficients

According to the computational formula given in Ref. 10, the SHG coefficients of BABO and KABO crystals were calculated from the bands energies and the wave functions. The factors that may influence the SHG coefficients include the number (or maximum energy) of empty bands and the *k* points used in calculation. In our previous paper, we concluded that the energy states in low conduction bands are much more important for SHG effects than those in higher bands through a series of tests. In addition, Duan *et al.* presented an evaluation technique to reduce the number of *k* points needed for convergence.[23] In Ref. 10, following Duan *et al.* we suggested an improved formula for SHG coefficients in which the calculation of SHG coefficients rapidly converges with not too many *k* points in the irreducible Brillouin zone (IBZ). For example, in the case of zinc-blende GaAs, conventional calculation needs 300–500*k* points in the IBZ to obtain convergence within 5%,[22] while using our improved formula convergence within 2% is achieved by use of only 28*k* points. In our present work, the electronic structure calculations of the above crystals are performed on the Γ point. After the ground-state-density calculation converges, finer *k* point sampling titled by denser *k* point sets[24] is reduced to 10 and 8 in the IBZ of the optical matrix element calculations for BABO and KABO, respectively. The cutoff energies are all 450 eV. This choice of *k* sampling and high enough cutoff energy leads to satisfactory convergence. Following these techniques, the theoretical SHG values are calculated and are listed in Table IV with experimental values. In order to calculate the respective contributions of cations and the anionic group to the SHG coefficients of crystals, we also adopt the real-space atom-cutting method. We have used the same atom-cutting radii mentioned in Sec. III B in the calculations of SHG coefficients. The decomposition results are also given in Table IV, in which the contributions of cations M^+ (M=K,Ba), and $(BO_3)^{3-}$ and $(AlO_4)^{5-}$ as well as their joint contributions are clearly seen. These calculated results lead to the following conclusions.

(i) Our plane-wave pseudopotential approach is also suitable for studying the SHG coefficients of borate crystals such as BABO and KABO. We see that the agreement between calculated and experimental values of the SHG coefficients is very good.

(ii) The contributions to the SHG coefficients from the anionic groups $(BO_3)^{3-}$ and $(AlO_4)^{5-}$ are beyond 90% for BABO and KABO. The SHG coefficients are almost a ''pure'' contribution of the anionic groups. In Table IV, it should be noted that the anionic group $(AlO_4)^{5-}$ gives a smaller contribution to the SHG coefficients than $(BO_3)^{3-}$ for BABO, but for KABO the contribution to SHG from the $(AlO_4)^{5-}$ is larger than that of $(BO_3)^{3-}$. The reasons are the following: $(AlO_4)^{5-}$ in BABO is a more approximate tetrahedron ($\angle$O–Al–O=102.0°, $\angle$bridged O–Al–O =115.6°), while in KABO the Al^{3+} and the three

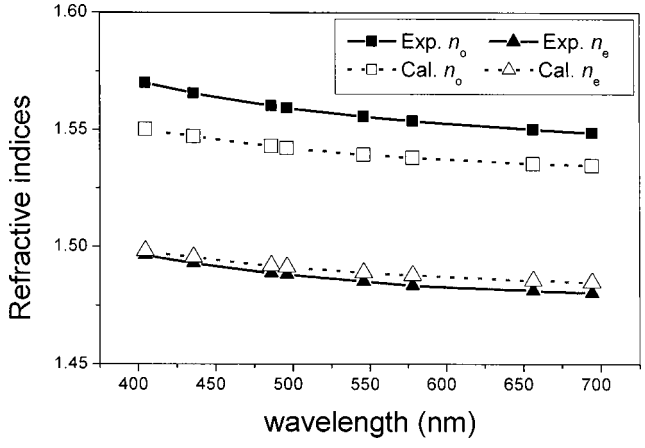

FIG. 5. Refractive index dispersion curve of KABO (experimental values from Ref. 4).

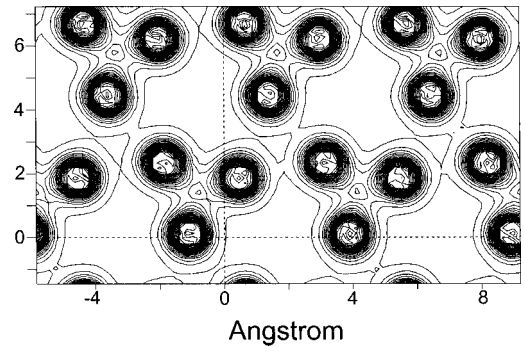

FIG. 6. Charge density in the $(BO_3)^{3-}$ group plane of BABO.

TABLE III. Comparison of refractive indices of BABO and KABO at the static limit derived from the atom-cutting method and original values

Crystal	Analysis	n_0	n_e	Δn
BABO	Origin	1.5757	1.5257	0.05
	BO_3^{3-} only	1.3423	1.2711	0.071
	AlO_4^{5-} only	1.3876	1.3818	0.006
	Ba^{2+} only	1.1616	1.1492	0.012
KABO	Origin	1.527	1.478	0.049
	BO_3^{3-} only	1.311	1.256	0.055
	AlO_4^{5-} only	1.367	1.349	0.018
	K^+ only	1.125	1.124	0.001

oxygen atoms except the bridged oxygen are more coplanar ($\angle$O–Al–O=115.6°, $\angle$bridged O–Al–O =102.3°). The deformation of $(AlO_4)^{5-}$ in KABO is larger than that of $(AlO_4)^{5-}$ in BABO, so their contributions to the SHG coefficients are larger. Moreover, the results of analysis of the SHG coefficients using the real-space atom-cutting method clearly show that with an increase in radius of the alkali and alkali-earth metal cations M^+ their contributions to the SHG coefficients become more and more significant in the same family of crystals. For example, only 1% of the d_{11} of KABO comes from the K^+ cation, while the contribution of the cation Ba^{2+} to d_{11} is approximately 12% for BABO. The result is the same as that of the BBO (Ref. 10) and LBO family.[11]

IV. CONCLUSION

An *ab initio* electronic/band-structures calculation was-carried out using the CASTEP package to study the optical properties of the SBBO family. Our investigations can be summarized as follows.

(i) The electronic and band structures of the above borate crystals were obtained. Due to the instability of the structure of SBBO, the electronic band structure of the crystal is not reliable, which consequently results in inaccuracy of the calculated optical coefficients.

TABLE IV. Calculated and experimental values of nonlinear susceptibilities of BABO and KABO crystals and analysis using the real-space atom-cutting method (in units of pm/V).

Crystal	d_{ij}	Calculated	Experiment	
BABO	d_{11}	0.745	0.75[a]	
KABO	d_{11}	−0.317	0.45[b]	
		Contribution		d_{ij}
BABO		Ba^{2+} only		0.115
		BO_3^{3-} only		0.348
		AlO_4^{5-} only		0.267
		Sum		0.730
KABO		K^+ only		0.012
		BO_3^{3-} only		−0.152
		AlO_4^{5-} only		−0.283
		Sum		−0.425

[a]Reference 3.
[b]Reference 4.

(ii) The DOS and PDOS reveal the compositions of each energy band. For BABO and KABO the tops of the valence band are almost dominated by the $2p$ of oxygen atoms. The conduction bands of the two crystals are mainly composed of valence $2p$ orbitals of B and O.

(iii) From the wave functions and band structures the linear and nonlinear optical coefficients were obtained for BABO and KABO. The calculated refractive indexes, birefringence, and SHG coefficients are in good agreement with experimental values. The analysis of results by the atom-cutting method reveals that the contributions from K^+ and Ba^{2+} to the refractive indices are comparable to those of anion groups $(BO_3)^{3-}$ and $(AlO_4)^{5-}$, but their contributions to the anisotropy of the refractive indices can be neglected. This means that the anisotropy of the refractive indices of the two crystals is mainly determined by the $(BO_3)^{3-}$ and $(AlO_4)^{5-}$ anionic groups. On the other hand, the more $(AlO_4)^{5-}$ is deformed, the more it contributes to the SHG coefficients. The contributions to the SHG coefficients from $(BO_3)^{3-}$ and $(AlO_4)^{5-}$ are beyond 95% for KABO, but with an increase of the radius of the M^+ cation their contributions to the SHG coefficients become more pronounced. As a result, for BABO crystal the contribution to the SHG coefficient from Ba^{2+} is beyond 12%. This conclusion is the same as that for the LBO family. We believe that further application of the real-space atom-cutting method may elucidate the origin of the optical effects, both linear and nonlinear. Such investigations will help us to find and design new NLO crystals more efficiently.

ACKNOWLEDGMENTS

This work was supported by the Chinese National Basic Research Project and by NSF Grant No. 90203016. Support in computing facilities from the Computer Network Information Center is gratefully acknowledged. LZS gratefully acknowledges the support of the K. C. Wang Education Foundation, Hong Kong. Another author (M.-H.L.) would like to express his thanks for funding support from NSC 89-211-M-032-026.

[1] C. T. Chen, N. Ye, J. Lin, J. Jiang, W. R. Zeng, and B. C. Wu, Adv. Mater. (Weinheim, Ger.) **11**, 1071 (1999).
[2] C. T. Chen, Y. B. Wang, B. C. Wu, K. V. Wu, W. R. Zeng, and L. H. Yu, Nature (London) **373**, 322 (1995).
[3] K. Yamada, Japan Kokai Tokyo Koho, Japanese Patent No. 09.61,864 (1994).
[4] N. Ye, W. Zeng, B. C. Wu, and C. Chen, Z. Kristallogr. - New Cryst. Struct. **213**, 452 (1998).
[5] N. Ye, W. Zeng, B. Wu, and C. Chen, Proc. SPIE **3556**, 21 (1998).
[6] Z. G. Hu, T. Higashiyama, M. Yoshimura, Y. Mori, and T. Sasaki, Z. Kristallogr. **214**, 433 (1999).
[7] J. A. Kaduk, L. C. Satek, and S. T. McKenna, Rigaku J. **16**, 17 (1999).
[8] J. H. Lu, G. L. Wang, Z. Y. Xu, C. T. Chen, J. Y. Wang, C. Q. Zhang, and Y. G. Liu, Chin. Phys. Lett. **19**, 680 (2002).
[9] CASTEP 3.5 program developed by Molecular Simulation Inc. (1997).
[10] J. Lin, M. H. Lee, Z. P. Liu, C. T. Chen, and C. J. Pickard, Phys. Rev. B **60**, 13380 (1999).

[11] Z. S. Lin, J. Lin, Z. Z. Wang, C. T. Chen, and M. H. Lee, Phys. Rev. B **62**, 1757 (2000).
[12] W. Kohn and L. J. Sham, Phys. Rev. **140**, 113 (1965).
[13] P. Perdew and Y. Wang, Phys. Rev. B **45**, 13244 (1992).
[14] R. G. Parr and W. T. Yang, *Density Functional Theory of Atom Molecules* (Oxford University Press, Oxford, 1989).
[15] M. C. Payne, K. M. Rabe, E. Kaxiras, and J. D. Joannopoulos, Phys. Rev. B **41**, 1227 (1993).
[16] A. M. Rappe, K. M. Rabe, E. Kaxiras, and J. D. Joannopoulos, Rev. Mod. Phys. **64**, 1045 (1992).
[17] J. S. Lin, A. Qtseish, M. C. Paye, and V. Heine, Phys. Rev. B **47**, 4174 (1993).
[18] M. H. Lee, J. S. Lin, M. C. Payne, V. Heine, V. Milman, and S. Crampin (unpublished).
[19] L. Kleinman and D. M. Bylander, Phys. Rev. Lett. **48**, 1425 (1982).
[20] R. W. Godby, M. Schluter, and L. J. Sham, Phys. Rev. B **37**, 10159 (1988).
[21] C. S. Wang and B. M. Klein, Phys. Rev. B **24**, 3417 (1981).
[22] S. N. Rashkeev, W. R. L. Lambrecht, and B. Segaall, Phys. Rev. B **57**, 3905 (1998).
[23] C. G. Duan, J. Li, Z. Q. Gu, and D. S. Wang, Phys. Rev. B **59**, 369 (1999).
[24] M. C. Payne, M. P. Teter, D. C. Allan *et al.*, Rev. Mod. Phys. **64**, 1045 (1992).